



## PREPRINT

# BWT construction and search at the terabase scale

Heng Li<sup>1,2,3,\*</sup>

<sup>1</sup>Department of Data Science, Dana-Farber Cancer Institute, 450 Brookline Ave, Boston, MA 02215, USA, <sup>2</sup>Department of Biomedical Informatics, Harvard Medical School, 10 Shattuck St, Boston, MA 02215, USA and <sup>3</sup>Broad Institute of MIT and Harvard, 415 Main St, Cambridge, MA 02142, USA

\*Corresponding author. [hli@ds.dfcf.harvard.edu](mailto:hli@ds.dfcf.harvard.edu)

## Abstract

**Motivation:** Burrows-Wheeler Transform (BWT) is a common component in full-text indices. Initially developed for data compression, it is particularly powerful for encoding redundant sequences such as pangenome data. However, BWT construction is resource intensive and hard to be parallelized, and many methods for querying large full-text indices only report exact matches or their simple extensions. These limitations have hampered the biological applications of full-text indices.

**Results:** We developed ropebwt3 for efficient BWT construction and query. Ropebwt3 could index 100 assembled human genomes in 21 hours and index 7.3 terabases of commonly studied bacterial assemblies in 26 days. This was achieved using 82 gigabytes of memory at the peak without working disk space. Ropebwt3 can find maximal exact matches and inexact alignments under affine-gap penalties, and can retrieve all distinct local haplotypes matching a query sequence. It demonstrates the feasibility of full-text indexing at the terabase scale.

**Availability and implementation:** <https://github.com/lh3/ropebwt3>

## 1. Introduction

Although millions of genomes have been sequenced, the majority of them were sequenced from a small number of species such as human, *E. coli* and *M. tuberculosis*. As a result, existing genome sequences are highly redundant. This is how Hunt et al. (2024) compressed 7.86 terabases (Tb) of bacterial assemblies, also known as AllTheBacteria, into 78.5 gigabytes (GB) after grouping phylogenetically related genomes (Břinda et al., 2024). The resultant compressed files losslessly keep all the sequences but are not directly searchable. Indexing is necessary to enable fast sequence search.

K-mer data structures are a popular choice for sequence indexing (Marchet et al., 2021). They can be classified into three categories. The first category does not associate k-mers with their positions in the database sequences. These data structures support membership query or pseudoalignment (Bray et al., 2016), but cannot reconstruct input sequences or report base alignment. Sequence search at petabase scale use all such methods (Edgar et al., 2022; Karasikov et al., 2024; Shiryev and Agarwala, 2024). The second category associates a subset of k-mers with their positions. Upon finding k-mer matches, algorithms in this category go back to the database sequences and perform base alignment. Most aligners work this way. However, because the database sequences are not compressed well, these algorithms may require large space to store them. The last category keeps all k-mers and their positions. Algorithms in this category can reconstruct all the database sequences without explicitly storing them. Nonetheless, although positions of k-mers can be compressed efficiently (Karasikov et al., 2020), they still take large space. The largest lossless k-mer index consists of a few terabases (Karasikov et al., 2024).

Compressed full-text indices, such as FM-index (Ferragina and Manzini, 2000) and r-index (Gagie et al., 2018; Bannai et al., 2020;

Gagie et al., 2020), provide an alternative way for fast sequence search (Navarro, 2022). The core component of these data structures is often Burrows-Wheeler Transform (BWT; Burrows and Wheeler 1994) which is a lossless transformation of strings. The BWT of a highly redundant string tends to group symbols in the original string into long runs and can thus be well compressed. When we supplement BWT with a data structure to efficiently compute the rank of a symbol in BWT, we can in theory count the occurrences of a string in time linear to its length. FM-index further adds a sampled suffix array to locate substrings, while r-index uses an alternative method that is more efficient for redundant strings. Both of them support compression and sequence search at the same time.

BWT-based indices have been used for read alignment (Langmead et al., 2009; Li and Durbin, 2009; Li et al., 2009), *de novo* sequence assembly (Simpson and Durbin, 2012) and data compression (Cox et al., 2012). They have also emerged as competent data structures for pangenome data. Existing pangenome-focused tools (Rossi et al., 2022; Ahmed et al., 2021; Zakeri et al., 2024) use prefix-free parsing for BWT construction (Boucher et al., 2019). They require more memory than input sequences and are impractical for huge datasets. Although ropebwt2 developed by us can construct BWT in memory proportional to its compressed size and is fast for short strings (Li, 2014), it is inefficient for chromosome-long sequences. OnlineRlbwt (Bannai et al., 2020) has a similar limitation. grlBWT (Díaz-Domínguez and Navarro, 2023) is likely the best algorithm for constructing the BWT of similar genomes. It reduces the peak memory at the cost of large working disk space and frequent disk input/output. In its current form, the algorithm does not support update to BWT. We would need to reconstruct the BWT from scratch when new genomes arrive. BWT construction for highly redundant sequences remains an active research area.

**Table 1.** Notations and naming convention

Notation	Description
$\Sigma$	Alphabet of symbols. $\{\mathbf{A}, \mathbf{C}, \mathbf{G}, \mathbf{T}, \mathbf{N}\}$ for DNA
$\Sigma'$	Augmented alphabet: $\Sigma' \triangleq \Sigma \cup \{\$\}$
$a, b, c$	Symbols in $\Sigma'$
$T$	Concatenated reference string including sentinels
$S(i)$	Suffix array: offset of the $i$ -th smallest suffix
$B$	BWT string: $B[i] \triangleq T[S(i) - 1]$
$m$	Number of sentinels: $m \triangleq  \{i : B[i] = \$\} $
$n$	Total length: $n \triangleq  T  =  B $
$r$	Number of runs: $r \triangleq  \{i : B[i] \neq B[i + 1]\}  + 1$
$C_B(a)$	Accumulative count: $C_B(a) \triangleq  \{i : B[i] < a\} $
$\text{rank}_B(a, k)$	Rank: $\text{rank}_B(a, k) \triangleq  \{i < k : B[i] = a\} $
$\pi(i)$	LF-mapping: $\pi(i) \triangleq S^{-1}(S(i) - 1)$

With BWT-based data structures, it is trivial to test the presence of string  $P$  in the index, but finding substring matches within  $P$  needs more thought. Learning from bidirectional BWT (Lam et al., 2009), we found a BWT constructed from both strands of DNA sequences supports the extension of exact matches in both directions (Li, 2012). This gave us an algorithm to compute maximal exact matches (MEMs), which was later improved by Gagie (2024) for long MEMs. Bannai et al. (2020) proposed a distinct algorithm to compute MEMs without requiring both strands. Matching statistics (Chang and Lawler, 1994) and pseudo-matching length (PML; Ahmed et al. 2021) have also been considered. All these algorithms find exact local matches only.

It is also possible to identify inexact local matches. With the BWT-SW algorithm, Lam et al. (2008) simulated a suffix trie, a tree data structure, with BWT and performed sequence-to-trie alignment to find all local matches between a query string and the BWT of a large genome. We went a step further by representing the query string with its direct acyclic word graph (DAWG; Blumer et al. 1983) and performed DAWG-to-trie alignment. This is the BWA-SW algorithm (Li and Durbin, 2010). Nonetheless, we later realized the formulation of BWA-SW had theoretical flaws and its implementation was closer to DAWG-to-DAWG alignment than to DAWG-to-tree alignment.

In this article, we will explain our solution to BWT construction and to sequence search at the terabase scale. Our contribution includes: a) a reinterpreted BWA-SW algorithm that fixes issues in our earlier work (Li and Durbin, 2010); b) its application in finding similar haplotypes; c) an incremental in-memory BWT construction implementation that scales to large pangenome datasets.

## 2. Methods

In a nutshell, ropebwt3 computes the partial multi-string BWT of a subset of sequences with libsaids and merges the partial BWT into the existing BWT run-length encoded as a B+-tree (Li, 2014). It repeats this procedure until all input sequences are processed. The BWT by default includes input sequences on both strands. This enables forward-backward search (Li, 2012) required by accelerated long MEM finding (Gagie, 2024). Ropebwt3 also reports local alignment with affine-gap penalty using a revised BWA-SW algorithm (Li and Durbin, 2010).

Ropebwt3 combines and adapts existing algorithms and data structures. Nonetheless, the notations here differ from our early work (e.g. from 1-based to 0-based coordinates) and from other publications. We will describe our methods in full for completeness.

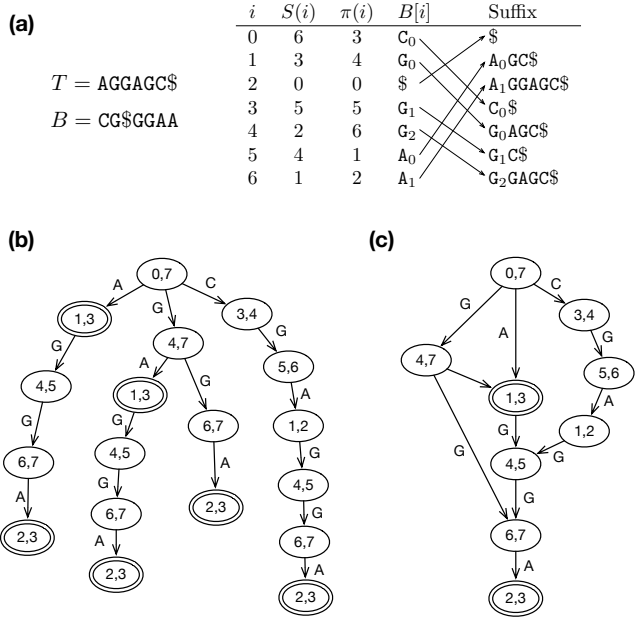


**Fig. 1.** Examples of BWT and related data structures. (a) The BWT  $B$ , suffix array  $S$  and LF-mapping  $\pi$  of string  $T$ . Subscripts are equal to the ranks of symbols in  $B$ , which are the same as the ranks among the suffixes (indicated by arrows). (b) The prefix trie simulated with BWT  $B$ . In each node, the pair of integers gives the suffix array interval of the string represented by the path from the node to the root. Double circles indicate nodes that can reach the beginning of  $T$ . (c) The prefix directed acyclic word graph (DAWG) of  $T$  by merging nodes with identical suffix array intervals.

### 2.1. Basic concepts

Let  $\Sigma$  be an alphabet of *symbols* (Table 1). Given a string  $P$  over  $\Sigma$ ,  $|P|$  is its length and  $P[i] \in \Sigma$ ,  $0 \leq i < |P|$ , is the  $i$ -th symbol in  $P$ , and  $P[i, j]$  is a substring of length  $j - i$  starting at  $i$ . Operator “ $\circ$ ” concatenates two strings or between strings and symbols. It may be omitted if concatenation is apparent from the context.

Suppose  $\mathcal{T} = (P_0, P_1, \dots, P_{m-1})$  is an ordered list of  $m$  strings over  $\Sigma$ .  $T \triangleq P_0 \$_0 P_1 \$_1 \dots P_{m-1} \$_{m-1}$  is the concatenation of the strings in  $\mathcal{T}$  with sentinels ordered by  $\$_0 < \$_1 < \dots < \$_{m-1}$ . For other ways to define string concatenation on ordered string lists or unordered string sets, see Cenzato and Lipták (2024).

For convenience, let  $n \triangleq |T|$  and  $T[-1] = T[n - 1]$ . The *suffix array* of  $T$  is an integer array  $S$  such that  $S(i)$ ,  $0 \leq i < n$ , is the start position of the  $i$ -th smallest suffix among all suffixes of  $T$  (Fig. 1a). The *Burrows-Wheeler Transform (BWT)* of  $T$  is a string  $B$  computed by  $B[i] = T[S(i) - 1]$ . All sentinels in  $B$  are represented by the same symbol “ $\$$ ” and are not distinguished from each other.  $\Sigma' \triangleq \Sigma \cup \{\$\}$  denotes the alphabet including the sentinel.

For  $a \in \Sigma'$ , let  $C_B(a) \triangleq |\{i : B[i] < a\}|$  be the number of symbols smaller than  $a$  and  $\text{rank}_B(a, k) \triangleq |\{i < k : B[i] = a\}|$  be the number of  $a$  before offset  $k$  in  $B$ . We may omit subscription  $B$  when we are describing one string only. The last-to-first mapping (*LF mapping*)  $\pi$  is defined by  $\pi(i) \triangleq S^{-1}(S(i) - 1)$ , where  $S^{-1}$  is the inverse function of suffix array  $S$ . It can be calculated as  $\pi(i) = C(B[i]) + \text{rank}(B[i], i)$ . As  $B[\pi(i)]$  immediately proceeds  $B[i]$  on  $T$ , we can use  $\pi$  to decode the  $i$ -th sequence in  $B$ .

### 2.2. BWT construction

Libsaids is an efficient library for computing the suffix array of a single string. It does not directly support a list of strings.

**Algorithm 1** Insert BWT  $B_2$  into BWT  $B_1$ 

```

1: procedure APPENDBWT( $B_1, B_2$ )
2:    $m_1 \leftarrow |\{k : B_1[k] = \$\}|$ ;  $m_2 \leftarrow |\{k : B_2[k] = \$\}|$ 
3:   for  $k \leftarrow 0$  to  $|B_2| - 1$  do
4:      $a \leftarrow B_2[k]$ 
5:      $R(k) \leftarrow (a, C_{B_2}(a) + \text{rank}_{B_2}(a, k))$ 
6:   end for
7:   for  $i \leftarrow 0$  to  $m_2 - 1$  do
8:      $k \leftarrow i$ ;  $l \leftarrow m_1$ 
9:     repeat
10:     $(a, k') \leftarrow R(k)$ 
11:     $R(k) \leftarrow (a, k + l)$      $\triangleright$  position in the merged BWT
12:     $k \leftarrow k'$ ;  $l \leftarrow C_{B_1}(a) + \text{rank}_{B_1}(a, l)$ 
13:   until  $a = \$$ 
14:   end for
15:   for  $(a, k) \in R$  do           $\triangleright$  N.B.  $k$  is sorted in array  $R$ 
16:     insert $_{B_1}(a, k)$            $\triangleright$  insert  $a$  after  $k$  symbols in  $B_1$ 
17:   end for
18: end procedure

```

Nonetheless, we note that  $T$  is a string over alphabet  $\Sigma'' = \{\$, \$_1, \dots, \$_{m-1}, A, C, G, T, N\}$  with lexicographical order  $\$_0 < \dots < \$_{m-1} < A < C < G < T < N$ . We can use  $m + 5$  non-negative integers to encode  $T$  and apply libsa. The suffix array derived this way will be identical to the suffix array of  $T$ .

For  $m$  that can be represented by a 32-bit integer and  $n$  represented by a 64-bit integer, libsa will need at least  $12n$  bytes to construct the suffix array. It is impractical for  $n$  more than tens of billions. To construct BWT for large  $n$ , ropebwt3 uses libsa to build the BWT for a batch (up to 7 Gb by default) and merges it to the BWT of already processed batches (Algorithm 1). The basic idea behind the algorithm is well known (Ferragina et al., 2010) but implementations vary (Sirén, 2016; Oliva et al., 2021). In ropebwt3, we encode BWT with a B+-tree (Fig. 2a). This yields  $O(\log r)$  rank query (line 12) and insertion (line 16), where  $r$  is the number of runs in the merged BWT. The bottleneck of the algorithm lies in rank calculation (line 7), which can be parallelized if  $m_2 > 1$ .

This online BWT construction algorithm does not use temporary disk space. The overall time complexity is  $O(n \log r)$ . The BWT takes  $O(r \log r)$  in space. The memory required for partial BWT construction with libsa depends on the batch size and the longest string. B+-tree is dynamic. Ropebwt3 optionally converts B+-tree to the fermi binary format (Fig. 2b; Li 2012) which is static but is faster to query and can be memory-mapped.

Ropebwt2 (Li, 2014) uses the same B+-tree to encode BWT and has the same time complexity. However, it inserts sequences, not partial BWTs, into existing BWT. It cannot be efficiently parallelized for long strings. Note that independent of our earlier work, Ohno et al. (2018) also used B+-tree to encode BWT. Its implementation (Bannai et al., 2020) is several times slower than ropebwt2 on 152 bacterial genomes from Li et al. (2024), possibly because ropebwt2 is optimized for the small DNA alphabet.

### 2.3. Suffix array interval and backward search

For a string  $P \in \Sigma^*$  (i.e. not including sentinels), let  $\text{occ}(P)$  be the number of occurrences of  $P$  in  $T$ . Define  $\text{lo}(P)$  to be the number of suffixes that lexicographically smaller than  $P$  and  $\text{hi}(P) \triangleq \text{lo}(P) + \text{occ}(P)$ .  $[\text{lo}(P), \text{hi}(P)]$  is called the *suffix array interval* of  $P$ , or *SA interval* in brief. An SA interval is *important* if there exists  $P$  such that it is the SA interval of  $P$ . The SA interval of the empty string is  $[0, n]$  where  $n = |T|$ . If we know the SA interval of  $P$ , we can

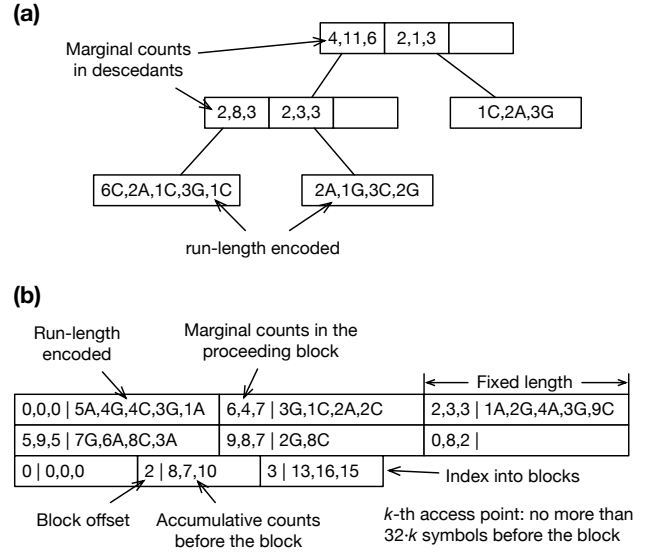


**Fig. 2.** Examples of binary BWT encoding. (a) Encoded as a B+-tree. An internal node keeps the marginal counts of symbols in its descendants. An external node keeps the run-length encoded substring in BWT. A run length may be encoded in one, two, four or eight bytes in a scheme inspired by UTF-8. (b) Encoded as a bit-packed array. The first two rows store run-length encoded BWT interleaved with marginal counts in each block. The Elias delta encoding is used to represent run lengths. The last row is an index into BWT for fast access.

calculate the SA interval of  $aP$  with:

$$\begin{aligned} \text{lo}(aP) &= C(a) + \text{rank}(a, \text{lo}(P)) \\ \text{hi}(aP) &= C(a) + \text{rank}(a, \text{hi}(P)) \end{aligned}$$

To calculate  $\text{occ}(P)$ , we can start with  $[0, n]$  and repeatedly apply the equation above from the last symbol in  $P$  to the first. This procedure is called *backward search*.

### 2.4. Double-strand BWT

The definitions above are applicable to generic strings. With one BWT, we can only achieve backward search; forward search additionally requires the BWT of the reverse strings (Lam et al., 2009). Nonetheless, due to the strand symmetry of DNA strings, it is possible to achieve both forward and backward search with one BWT provided that the BWT contains both strands of DNA strings (Li, 2012).

Formally, a DNA alphabet is  $\Sigma = \{A, C, G, T, N\}$ .  $\bar{a}$  denotes the Watson-Crick complement of symbol  $a \in \Sigma$ . The complement of  $\$, A, C, G, T$  and  $N$  are  $\$, T, G, C, A$  and  $N$ , respectively.

For string  $P$ ,  $\bar{P}$  is its reverse complement string. The double-strand concatenation of a DNA string list  $\mathcal{T} = (P_0, P_1, \dots, P_{m-1})$  is  $\tilde{\mathcal{T}} = P_0 \$_0 \bar{P}_0 \$_1 P_1 \$_2 \bar{P}_1 \$_3 \dots P_{m-1} \$_{2m-2} \bar{P}_{m-1} \$_{2m-1}$ . The *double-strand BWT* (DS-BWT) of  $\mathcal{T}$  is the BWT of  $\tilde{\mathcal{T}}$ . We note that if  $P$  is a substring of  $\tilde{\mathcal{T}}$ ,  $\bar{P}$  must be a substring and  $\text{occ}(P) = \text{occ}(\bar{P})$ . The *suffix array bidirectional interval* (SA bi-interval) of  $P$  is a 3-tuple defined as  $(\text{lo}(P), \text{lo}(\bar{P}), \text{occ}(P))$ .

An SA bi-interval can be extended in both backward and forward directions. To calculate the SA bi-interval of  $aP$ , we can use the standard backward search to compute  $\text{lo}(aP)$  and  $\text{occ}(aP)$  from  $\text{lo}(P)$  and  $\text{occ}(P)$ . As to  $\text{lo}(\bar{aP})$ , we note that  $[\text{lo}(\bar{aP}), \text{hi}(\bar{aP})] \subset [\text{lo}(\bar{P}), \text{hi}(\bar{P})]$  because  $\bar{aP} = \bar{P} \circ \bar{a}$  is prefixed with  $\bar{P}$ . We can thus calculate  $\text{lo}(\bar{aP}) = \text{lo}(\bar{P}) + \sum_{b < \bar{a}} \text{occ}(\bar{P}b) = \text{lo}(\bar{P}) + \sum_{b < \bar{a}} \text{occ}(\bar{bP})$ .

**Algorithm 2** Backward and forward extensions with DS-BWT

```

1: procedure BACKWARDEXT( $B, (k, k', s), a$ )
2:   for all  $b < \bar{a}$  do                                 $\triangleright b$  can be $ 
3:      $k' \leftarrow k' + [\text{rank}(\bar{b}, k + s) - \text{rank}(\bar{b}, k)]$ 
4:   end for
5:    $s \leftarrow \text{rank}(a, k + s) - \text{rank}(a, k)$ 
6:    $k \leftarrow C(a) + \text{rank}(a, k)$ 
7:   return  $(k, k', s)$ 
8: end procedure
9: procedure FORWARDEXT( $B, (k, k', s), a$ )
10:   $(k', k, s) \leftarrow \text{BACKWARDEXT}(B, (k', k, s), \bar{a})$ 
11:  return  $(k, k', s)$ 
12: end procedure

```

It is easy to see that if  $(k, k', s)$  is the SA bi-interval of  $P$ ,  $(k', k, s)$  is the SA bi-interval of  $\bar{P}$ , and vice versa. Therefore, we can use the backward extension of  $\bar{P}$  to achieve the forward extension of  $P$ . Algorithm 2 gives the details. It simplifies the original formulation (Li, 2012).

**2.5. Finding supermaximal exact matches**

An *exact match* between string  $T$  and  $P$  is a 3-tuple  $(l, t, p)$  such that  $T[t, t + l] = P[p, p + l]$ . A *maximal exact match* (MEM) is an exact match that cannot be extended in either direction. A MEM may be contained in another MEM on the pattern string  $P$ . For example, suppose  $T = \text{GACCTCCG}$  and  $P = \text{ACCT}$ . MEM  $(2, 6, 1)$  is contained in MEM  $(4, 1, 0)$  on the pattern string. A *supermaximal exact match* (SMEM) is a MEM that is not contained in other MEMs on the pattern string. In the example above, only  $(4, 1, 0)$  is a SMEM. There are usually much fewer SMEMs than MEMs. Gagie (2024) recently proposed a new algorithm to find long SMEMs (Algorithm 3) that is faster than our earlier algorithm (Li, 2012) especially when there are many short SMEMs to skip. Both algorithms can also find SMEMs occurring at least  $s_{\min}$  times (Tatarnikov et al., 2023).

**Algorithm 3** Finding SMEMs no shorter than  $\ell$  (Gagie, 2024)

```

1: procedure FINDSMEM1( $\ell, s_{\min}, B, P, i$ )
2:   if  $i + \ell > |P|$  then return  $|P|$      $\triangleright$  Reaching the end of  $|P|$ 
3:    $(k, k', s) \leftarrow (0, 0, |B|)$          $\triangleright$  SA bi-interval of empty string
4:   for  $j \leftarrow i + \ell - 1$  to  $i$  do           $\triangleright$  backward
5:      $(k, k', s) \leftarrow \text{BACKWARDEXT}(B, (k, k', s), P[j])$ 
6:     if  $s < s_{\min}$  then return  $j + 1$ 
7:   end for
8:   for  $j \leftarrow i + \ell$  to  $|P| - 1$  do     $\triangleright$  forward
9:      $(k, k', s) \leftarrow \text{FORWARDEXT}(B, (k, k', s), P[j])$ 
10:    if  $s < s_{\min}$  then break
11:   end for
12:    $e \leftarrow j$  and output  $[i, e]$            $\triangleright$  SMEM found
13:    $(k, k', s) \leftarrow (0, 0, |B|)$ 
14:   for  $j \leftarrow e$  to  $i + 1$  do         $\triangleright$  backward again
15:      $(k, k', s) \leftarrow \text{BACKWARDEXT}(B, (k, k', s), P[j])$ 
16:     if  $s < s_{\min}$  then return  $j + 1$ 
17:   end for
18: end procedure
19: procedure FINDSMEM( $\ell, s_{\min}, B, P$ )
20:    $i \leftarrow 0$ 
21:   repeat
22:      $i \leftarrow \text{FINDSMEM1}(\ell, s_{\min}, B, P, i)$ 
23:   until  $i \geq |P|$ 
24: end procedure

```

**Algorithm 4** The revised BWA-SW algorithm

```

1: procedure BWASW( $G_P, G_T$ )
2:   for  $u \in V(G_P)$  in topological order do
3:     for  $u' \in \text{pre}(u)$  do                 $\triangleright$  predecessors of  $u$ 
4:       for  $v' \in V(G_T)$  s.t.  $H_{u'v'} > 0$  do     $\triangleright$  match
5:         for  $v \in \text{child}(v')$  do           $\triangleright$  children of  $v'$ 
6:            $H_{uv} \leftarrow \max\{H_{uv}, H_{u'v'} + s(u', u; v', v)\}$ 
7:         end for
8:       end for
9:       for  $v \in V(G_T)$  s.t.  $H_{u'v} > 0$  do     $\triangleright$  insertion
10:         $E_{uv} \leftarrow \max\{E_{uv}, \max\{H_{u'v} - q, E_{u'v}\} - e\}$ 
11:         $H_{uv} \leftarrow \max\{H_{uv}, E_{uv}\}$ 
12:      end for
13:    end for
14:    for  $v' \in V(G_T)$  s.t.  $H_{uv'} > 0$  do     $\triangleright$  deletion
15:      for  $v \in \text{child}(v')$  do           $\triangleright$  children of  $v'$ 
16:         $F_{uv} \leftarrow \max\{F_{uv}, \max\{H_{uv'} - q, F_{uv'}\} - e\}$ 
17:         $H_{uv} \leftarrow \max\{H_{uv}, F_{uv}\}$ 
18:      end for
19:    end for
20:  end for
21: end procedure

```

**2.6. Finding inexact matches**

The prefix trie of  $T$  is a tree that encodes all the prefixes of  $T$  (Fig. 1b). Each edge in the tree is labeled with a symbol in  $\Sigma$ . A path from a node to the root spells a substring of  $T$ . We can label a node with the SA interval of the string from the node to the root. When we know the label of a node, we can find the label of its child using backward search. We can thus simulate the top-down traversal of the prefix trie (Lam et al., 2008).

As is shown in Fig. 1b, different nodes in the prefix trie may have the same label. If we merge nodes with the same label (Fig. 1c), we will get a prefix DAWG (Blumer et al., 1983). For  $|T| > 1$ , the DAWG has at most  $2|T| - 1$  nodes (Blumer et al., 1984). Each node uniquely corresponds to an important SA interval of  $T$ .

Let  $G_T$  denote the prefix DAWG of  $T$  and  $V(G_T)$  be the set of vertices in  $G_T$ . Given a reference string  $T$  and a pattern string  $P$ , we can align  $G_T$  and  $G_P$  under affine-gap penalty with

$$\left\{ \begin{array}{l} E_{uv} = \max_{u' \in \text{pre}(u)} \{ \max\{H_{u'v} - q, E_{u'v}\} \} - e \\ F_{uv} = \max_{v' \in \text{pre}(v)} \{ \max\{H_{uv'} - q, F_{uv'}\} \} - e \\ G_{uv} = \max_{u' \in \text{pre}(u), v' \in \text{pre}(v)} \{ H_{u'v'} + s(u', u; v', v) \} \\ H_{uv} = \max\{G_{uv}, E_{uv}, F_{uv}\} \end{array} \right.$$

where  $u \in V(G_P)$ ,  $v \in V(G_T)$ ,  $\text{pre}(u)$  and  $\text{pre}(v)$  are the sets of predecessors in  $G_P$  and  $G_T$  respectively,  $q$  is the gap open penalty,  $e$  is the gap extension penalty, and  $s(u', u; v', v)$  is the match/mismatch score between the symbol labeled on edge  $(u', v)$  in  $G_P$  and the symbol on  $(v', v)$  in  $G_T$ . This equation is similar to but not the same as our earlier result (Li and Durbin, 2010).

On real data,  $G_T$  may be too large to store explicitly. Ropebwt3 instead explicitly stores  $G_P$  only and traverses it in the topological order (Algorithm 4). At a node  $u \in V(G_P)$ , we use a hash table to keep  $\{v \in V(G_T) : H_{uv} > 0\}$ . This algorithm is exact in that it guarantees to find the best alignment. In practice, however, a large number of  $v \in V(G_T)$  may be aligned to  $u$  with  $H_{uv} > 0$ . It is slow and memory demanding to keep track of all cells  $(u, v)$  with positive scores when  $P$  is long. Similar to our earlier work, we only store top  $W$  cells (25 by default) at each  $u$ . This heuristic is akin to dynamic banding for linear sequences (Suzuki and Kasahara, 2018).

## 2.7. Estimating local haplotype diversity

BWA-SW with the banding heuristic may miss the best matching haplotype especially given an index consisting of similar haplotypes. When the suffix on the best full-length alignment has a lot more mismatches than the suffix on suboptimal alignments, the best alignment may have moved out of the band early in the iteration and thus get missed. Nevertheless, a long read sequenced from a new sample may be the recombinant of two genomes in the index. We often do not seek the best alignment of the long read to a single haplotype. We are instead more interested in the collection of haplotypes a query sequence can be aligned to even if they do not lead to the best alignment. This now becomes possible as BWA-SW explores suboptimal alignments to multiple haplotypes.

More exactly, we perform semi-global sequence-to-DAWG alignment (i.e. requiring the query sequence to be aligned from end to end) by applying BWA-SW to the graph of the linear query sequence  $P$ . We can find the set of matching haplotypes  $\mathcal{M} \triangleq \{v \in V(G_T) : H_{u_0}v > 0\}$  where  $u_0$  represents the start of  $P$ .  $\mathcal{M}$  may include suboptimal haplotypes caused by small variants as well as the optimal one. Importantly,  $P$  may be aligned to similar positions on  $T$  with slightly different gap placements and alignment scores. In theory, we can identify this case by locating the position of each alignment. This procedure is slow as the “locate” operation is costly. We instead leverage the bi-directionality to identify redundancy heuristically. Suppose  $P$  can be aligned to SA bi-intervals  $(k_1, k'_1, s_1)$  and  $(k_2, k'_2, s_2)$  and the alignment score to the first interval is higher. We filter out the second interval if  $[k_2, k_2 + s_2) \subset [k_1, k_1 + s_1)$  or  $[k'_2, k'_2 + s_2) \subset [k'_1, k'_1 + s_1)$ .

In practice, we may apply this algorithm to the flanking sequence of a variant or to sliding k-mers of a long query sequence to enumerate possible local haplotypes and estimate their frequencies in the index. It is a new query type that is biologically meaningful.

## 3. Results

### 3.1. Performance on index construction

We evaluated the performance of BWT construction on 100 haplotype-resolved human assemblies collected in [Li et al. \(2024\)](#). As we included both strands (Section 2.4), each BWT construction algorithm took about 600 billion as input. The average run length is 141.6. grlBWT (commit 5b6d26a; [Díaz-Domínguez and Navarro 2023](#)) is the fastest algorithm (Table 2) at the cost of more than a terabyte of working disk space including decompressed sequences. Ropebwt3 took 21 hours from input sequences in gzip'd FASTA to the final index. It does not use working disk space and can append new sequences to an existing BWT. However, hardcoded for the DNA alphabet, ropebwt3 does not work with more general

**Table 2.** Indexing performance

Dataset	Algorithm	Elapsed <sup>1</sup>	CPU <sup>1</sup>	RAM
human100	grlBWT	8.3 h	29.6 h	84.8 GB
	pfp-thres <sup>2</sup>	51.7 h	51.5 h	788.1 GB
	ropebwt3	20.5 h	469.4 h	83.0 GB
	metagraph <sup>3</sup>	16.9 h	314.8 h	251.0 GB
	fulgor <sup>4</sup> (lossy)	1.2 h	32.7 h	165.2 GB
CommonBacteria	ropebwt3	26.5 d	830.3 d	67.3 GB

<sup>1</sup>Up to 64 threads specified if multi-threading is supported.

<sup>2</sup>excluding time for format conversion; “h” for hours; “d” for days

<sup>3</sup>pfp-thresholds was run on a slower machine with more RAM

<sup>4</sup>k-mer coordinates in the “row\_diff\_brwt\_coord” encoding

<sup>4</sup>without “--meta --diff” as the basic index is smaller; lossy index

**Table 3.** Query performance

Data	Algorithm	Type <sup>4</sup>	Speed <sup>5</sup> (kb/s)	RAM (GB)
SR+ <sup>1</sup>	ropebwt3	MEM31	1758.5	10.6
		MEM51	1907.5	10.6
		SW10	84.1	15.2
	MONI <sup>6</sup>	MEM-	453.2	68.4
		extend	348.2	68.4
		Movi	5894.0	47.6
		metagraph	PA+	<0.1
		fulgor	PA	2717.5
	LR+ <sup>2</sup>	MEM31	1695.9	10.5
		MEM51	1793.9	10.5
		SW25	82.7	15.6
LR- <sup>3</sup>	MONI	MEM-	413.6	68.4
		Movi	16204.9	47.6
		metagraph	PA+	<0.1
	fulgor	PA	2491.6	5.1
		ropebwt3	MEM31	1365.0
		MEM51	3051.6	10.4
		SW25	58.2	17.9
		MONI	MEM-	186.8
	Movi	PML	8490.9	47.6
		metagraph	PA+	1119.3
		fulgor	PA	4240.8

<sup>1</sup>first 1 million 125bp human short reads from SRR3099549

<sup>2</sup>first 10,000 human PacBio HiFi reads from SRR26545347

<sup>3</sup>first 10,000 metagenomic PacBio HiFi reads from DRR290133

<sup>4</sup>MEMx: super-maximal exact matches (SMEMs) of  $x$  bp or longer with counts; MEM-: SMEM without counts; extend: Smith-Waterman extension from the longest SMEM; PML: pseudo-matching length; PA: pseudo-alignment; PA+: pseudo-alignment with contig names; SWy: BWA-SW with bandwidth  $y$

<sup>5</sup>kilobases processed per CPU second. Index loading time excluded

<sup>6</sup>The MONI index includes both strands. We modified MONI such that extension is performed on the forward query strand only

alphabets. pfp-thresholds ([Rossi et al. 2022](#)) used more memory than the input sequences. It may be impractical with increased sample size.

Both MONI (v0.2.1; [Rossi et al. 2022](#)) and Movi (v1.1.0; [Zakeri et al. 2024](#)) use pfp-thresholds for building BWT. They generate additional data structures on top of BWT. Time spent on these additional steps were not counted. The tested version of Movi used more than one terabyte of memory to construct the final index. The Movi developer kindly provided the Movi index for the evaluation of query performance in the next section.

We also indexed the same dataset with k-mer based tools. In the lossless mode, metagraph (v0.3.6; [Karasikov et al. 2024](#)) indexed the 100 human genomes in 17 hours (Table 2). Fulgor (v3.0.0; [Fan et al. 2024](#)) is by far the fastest. However, lossy in nature, it is not directly comparable to the rest of the tools in the table.

To test the scalability of ropebwt3 in preparation for larger incoming pangenome datasets, we constructed the BWT of AllTheBacteria ([Hunt et al. 2024](#)) excluding the “dustbin” and “unknown” categories that include relatively unique genomes. This subset, which we call as CommonBacteria, consists of 278.4 million sequences in 7.33 Tb. An older version of ropebwt3 took less than a month to construct the double-strand BWT with 15.66 trillion symbols. We expect the latest version to reduce the elapsed time to about 17 days. The final index in the fermi format is 27.6 GB in size. Indexing the entire AllTheBacteria dataset will probably take 100–200 GB as unique sequences are not compressed well.

### 3.2. Query performance

We queried 100–200 Mb human short reads (SR+), human long reads (LR+) and non-human long reads (LR-) against the human pangenome indices constructed above (Table 3). It is important to note that no two tools support exactly the same type of query, but the comparison can still give a hint about the relative performance.

Among the three BWT-based tools, ropebwt3 is slower than Movi but faster than MONI on finding exact matches. Movi finds pseudo-matching length (PML). Although the fastest, it finds the longest exact matches for only 195 out of one million short reads and it misses the longest exact matches for all long reads. The longest PML of each read is on average 27% shorter than the longest exact match for LR+ and 22% shorter for SR+. Nonetheless, we believe it should be possible to implement SMEM finding based on the Movi data structure with a minor performance overhead.

MONI and ropebwt3 can also find inexact matches. Implementing r-index, MONI can relatively cheaply locate one SMEM. It leverages this property to extract the genomic sequence around the longest SMEM and performs Smith-Waterman extension. MONI extension is faster than BWA-SW on SR+ because it does not need to inspect suboptimal hits. This feature apparently focuses on short reads only. On LR+, MONI extension fails to extend to the ends of reads and generate incorrect output for the majority of reads.

As to k-mer indices, fulgor outputs the labels of genomes that each read have enough 31-mer matches to. In its current form, such output is not useful for pangome analysis as we know most of reads can be mapped to all genomes. Metagraph can additionally output the contig name of each match. However, when most k-mers are present in the index, metagraph is impractically slow.

### 3.3. Identifying novel sequences

As a biological application, we used the pangome index to identify novel sequences in reads that are absent from other human genomes. For this, we downloaded the PacBio HiFi reads for tumor sample COLO829 (<https://downloads.pacbcloud.com/public/revio/2023Q2/COL0829/COL0829/>), mapped them to the pangome index with 100 human genomes and extracted  $\geq 1\text{kb}$  regions on reads that are not covered by SMEMs of 51bp or longer. We found 95kb sequences in 43 reads. These sequences could not be assembled. NCBI BLAST suggested multiple weak hits to cow genomes. We could not identify the source of these sequences but there were few of them anyway.

When we mapped the COLO829 reads to a single T2T-CHM13 genome (Nurk et al., 2022) and applied the same procedure, we found 55.9Mb of “novel” sequences in 25,365 reads. The much larger number is probably caused by regions with dense SNPs that prevented long exact matches. Counterintuitively, mapping these reads to T2T-CHM13 with minimap2 (Li, 2018) resulted in more “novel” sequences at 78.6Mb, probably because minimap2 ignores seeds occurring thousands of times in T2T-CHM13 and may miss more alignments. Capable of finding SMEMs at the pangome scale, ropebwt3 is more effective for identifying known sequences. It is also faster than full minimap2 alignment against a single genome.

### 3.4. Haplotype diversity around C4 genes

The reference human genome GRCh38 has two paralogous C4 genes, *C4A* and *C4B*, and they may have copy-number changes (Sekar et al., 2016). In both cases, the exon 26 harbors the functional domain. We extracted the exon 26 from both genes from GRCh38. They differ at six mismatches over 157bp. We aligned both 157bp segments, one from each gene, to the human pangome. 105 haplotypes have the same *C4A* exon 26 sequence, one haplotype has a mismatch at offset 128 and four haplotypes have a mismatch

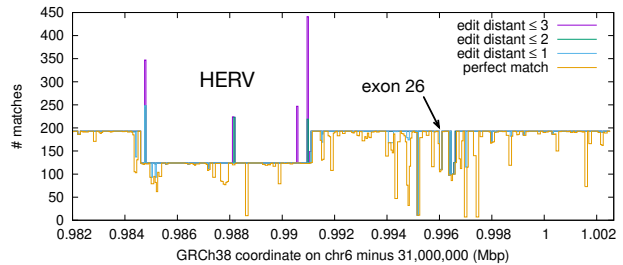


**Fig. 3.** Haplotype diversity around the *C4A* gene. 101-mers with 50bp overlaps are extracted from the *C4A* genomic sequence on GRCh38 and aligned to the human pangome. The Y axis shows the count of a 101-mer matches under different edit-distance thresholds.

at 54. In case of *C4B*, 60 haplotypes have the same reference *C4B* sequence and 23 also have a mismatch at offset 54. This means among the 100 human haplotypes, there are 110 *C4A* gene copies and 83 *C4B* copies. If we increase the bandwidth from the default 25 to 200, BWA-SW will be able to align *C4A* exon 26 to *C4B* genes and output all five hits for each sequence.

Fig. 3 shows the local haplotype diversity across the entire *C4A* gene spanning  $\sim 20.6\text{kb}$  on GRCh38. We can see most regions have 193 copies, except a  $\sim 6.4\text{kb}$  HERV insertion that separates long and short forms (Sekar et al., 2016). The dip around exon 26 is caused by the *C4A*–*C4B* difference. We could only see these alternative haplotypes with BWA-SW which reports suboptimal hits.

## 4. Discussions

Ropebwt3 is a fast tool for BWT construction and sequence search for redundant DNA sequences. Generating BWT purely in memory and supporting incremental build, ropebwt3 is convenient and practical for BWT construction at large scale. It provides the fastest algorithm so far for finding supermaximal exact matches and can report inexact hits as well. Ropebwt3 demonstrates that BWT-based data structures are scalable to terabases of pangome data.

Ropebwt3 will take 2–3 weeks to index 1,000 human genomes assembled from long reads. When there are more genomes, it will be faster to construct the BWT of individual genome independently and then merge them one by one. This strategy will use working disk space but achieve better parallelization. Sirén (2016) introduced disk-based algorithms for merging large BWTs, which may further improve the parallelization of BWT merge.

We thought about implementing r-index in ropebwt3. However, although an r-index is faster than an FM-index of the same size, it imposes a fixed sampling rate: two suffix array values per run. The BWT of CommonBacteria has 14.6 trillion bases and 17.6 billion runs. An r-index is likely to take more than 200GB, while an FM-index sampled at one position per 8,192bp takes 17.5GB in ropebwt3. We are still looking for a more balanced algorithm for the “locate” operation.

We often use pangome graphs to analyze multiple similar genomes (Liao et al., 2023). These graphs are built from the multiple sequence alignment through complex procedures involving many parameters (Li et al., 2020; Hickey et al., 2023; Garrison et al., 2023). It is challenging to understand if the graph topology is biologically meaningful especially given that we do not know the correct alignment between two genomes, let alone multiple ones. Complement to graph-based data structures, BWT-based algorithms are often exact with no heuristics or parameters but they tend to support limited query types. For example, we cannot

project the alignment to a designated reference genome. What additional query types we can achieve will be of great interest to the comprehensive pangenome analysis in future.

## Acknowledgments

We are grateful to Travis Gagie for pointing us to his long MEM finding algorithm, to Ilya Grebnov for adding the support of 16-bit alphabet which helps to accelerate ropebwt3, to Mohsen Zakeri for providing the Movi index, to Massimiliano Rossi for explaining the MONI algorithm, and to Giulio Pibiri and Rob Patro for troubleshooting compilation issues with fulgor.

## Author contributions

H.L. conceived the project, implemented the algorithms, analyzed the data and drafted the manuscript.

## Conflict of interest

None declared.

## Funding

This work is supported by National Institute of Health grant R01HG010040 and U01HG010961 (to H.L.).

## Data availability

The ropebwt3 source code is available at <https://github.com/lh3/ropebwt3>. Prebuilt ropebwt3 indices can be obtained from <https://zenodo.org/doi/10.5281/zenodo.11533210>.

## References

Ahmed, O., Rossi, M., Kovaka, S., Schatz, M. C., Gagie, T., et al. (2021). Pan-genomic matching statistics for targeted nanopore sequencing. *iScience*, 24:102696.

Bannai, H., Gagie, T., and I, T. (2020). Refining the  $r$ -index. *Theor. Comput. Sci.*, 812:96–108.

Blumer, A., Blumer, J., Ehrenfeucht, A., Haussler, D., and McConnell, R. M. (1983). Linear size finite automata for the set of all subwords of a word - an outline of results. *Bull. EATCS*, 21:12–20.

Blumer, A., Blumer, J., Ehrenfeucht, A., Haussler, D., and McConnell, R. M. (1984). Building the minimal DFA for the set of all subwords of a word on-line in linear time. In Paredaens, J., editor, *Automata, Languages and Programming, 11th Colloquium, Antwerp, Belgium, July 16–20, 1984, Proceedings*, volume 172 of *Lecture Notes in Computer Science*, pages 109–118. Springer.

Boucher, C., Gagie, T., Kuhnle, A., Langmead, B., Manzini, G., and Mun, T. (2019). Prefix-free parsing for building big BWTs. *Algorithms Mol Biol*, 14:13.

Bray, N. L., Pimentel, H., Melsted, P., and Pachter, L. (2016). Near-optimal probabilistic RNA-seq quantification. *Nat Biotechnol*, 34:525–7.

Břinda, K., Lima, L., Pignotti, S., Quinones-Olvera, N., Salikhov, K., et al. (2024). Efficient and robust search of microbial genomes via phylogenetic compression. *bioRxiv*.

Burrows, M. and Wheeler, D. J. (1994). A block sorting lossless data compression algorithm. Technical report 124, Digital Equipment Corporation.

Cenzato, D. and Lipták, Z. (2024). A survey of BWT variants for string collections. *Bioinformatics*, 40:btae333.

Chang, W. I. and Lawler, E. L. (1994). Sublinear approximate string matching and biological applications. *Algorithmica*, 12:327–344.

Cox, A. J., Bauer, M. J., Jakobi, T., and Rosone, G. (2012). Large-scale compression of genomic sequence databases with the Burrows-Wheeler transform. *Bioinformatics*, 28:1415–9.

Díaz-Domínguez, D. and Navarro, G. (2023). Efficient construction of the BWT for repetitive text using string compression. *Inf. Comput.*, 294:105088.

Edgar, R. C., Taylor, B., Lin, V., Altman, T., Barbera, P., et al. (2022). Petabase-scale sequence alignment catalyses viral discovery. *Nature*, 602:142–147.

Fan, J., Khan, J., Singh, N. P., Pibiri, G. E., and Patro, R. (2024). Fulgor: a fast and compact k-mer index for large-scale matching and color queries. *Algorithms Mol Biol*, 19:3.

Ferragina, P., Gagie, T., and Manzini, G. (2010). Lightweight data indexing and compression in external memory. In López-Ortiz, A., editor, *LATIN*, volume 6034, pages 697–710. Springer.

Ferragina, P. and Manzini, G. (2000). Opportunistic data structures with applications. In *FOCS*, pages 390–398. IEEE Computer Society.

Gagie, T. (2024). How to find long maximal exact matches and ignore short ones. In Day, J. D. and Manea, F., editors, *Developments in Language Theory - 28th International Conference, DLT 2024, Göttingen, Germany, August 12–16, 2024, Proceedings*, volume 14791 of *Lecture Notes in Computer Science*, pages 131–140. Springer.

Gagie, T., Navarro, G., and Prezza, N. (2018). Optimal-time text indexing in bwt-runs bounded space. In Czumaj, A., editor, *Proceedings of the Twenty-Ninth Annual ACM-SIAM Symposium on Discrete Algorithms, SODA 2018, New Orleans, LA, USA, January 7–10, 2018*, pages 1459–1477. SIAM.

Gagie, T., Navarro, G., and Prezza, N. (2020). Fully functional suffix trees and optimal text searching in BWT-runs bounded space. *J. ACM*, 67:2:1–2:54.

Garrison, E., Guerracino, A., Heums, S., et al. (2023). Building pangenome graphs. *bioRxiv*.

Hickey, G., Monlong, J., Ebler, J., et al. (2023). Pangenome graph construction from genome alignments with Minigraph-Cactus. *Nat Biotechnol*.

Hunt, M., Lima, L., Shen, W., Lees, J., and Iqbal, Z. (2024). AllTheBacteria - all bacterial genomes assembled, available and searchable. *bioRxiv*.

Karasikov, M., Mustafa, H., Danciu, D., Zimmermann, M., Barber, C., et al. (2024). Indexing all life's known biological sequences. *bioRxiv*.

Karasikov, M., Mustafa, H., Joudaki, A., Javadzadeh-No, S., Rätsch, G., and Kahles, A. (2020). Sparse binary relation representations for genome graph annotation. *J Comput Biol*, 27:626–639.

Lam, T. W., Li, R., Tam, A., Wong, S. C. K., Wu, E., and Yiu, S. (2009). High throughput short read alignment via bi-directional BWT. In *2009 IEEE International Conference on Bioinformatics and Biomedicine, BIBM 2009, Washington, DC, USA, November 1–4, 2009, Proceedings*, pages 31–36. IEEE Computer Society.

Lam, T. W., Sung, W. K., Tam, S. L., Wong, C. K., and Yiu, S. M. (2008). Compressed indexing and local alignment of DNA. *Bioinformatics*, 24:791–7.

Langmead, B., Trapnell, C., Pop, M., and Salzberg, S. L. (2009). Ultrafast and memory-efficient alignment of short dna sequences to the human genome. *Genome Biol*, 10:R25.

Li, H. (2012). Exploring single-sample SNP and INDEL calling with whole-genome de novo assembly. *Bioinformatics*, 28:1838–44.

Li, H. (2014). Fast construction of FM-index for long sequence reads. *Bioinformatics*, 30:3274–5.

Li, H. (2018). Minimap2: pairwise alignment for nucleotide sequences. *Bioinformatics*, 34:3094–3100.

Li, H. and Durbin, R. (2009). Fast and accurate short read alignment with Burrows-Wheeler Transform. *Bioinformatics*, 25:1754–60.

Li, H. and Durbin, R. (2010). Fast and accurate long-read alignment with Burrows-Wheeler transform. *Bioinformatics*, 26:589–95.

Li, H. et al. (2020). The design and construction of reference pangenome graphs with minigraph. *Genome Biol*, 21:265.

Li, H., Marin, M., and Farhat, M. R. (2024). Exploring gene content with pangene graphs. *Bioinformatics*, 40:btae456.

Li, R., Yu, C., Li, Y., Lam, T.-W., Yiu, S.-M., et al. (2009). SOAP2: an improved ultrafast tool for short read alignment. *Bioinformatics*, 25:1966–7.

Liao, W.-W., Asri, M., Ebler, J., Doerr, D., Haukness, M., et al. (2023). A draft human pangenome reference. *Nature*, 617:312–324.

Marchet, C., Boucher, C., Puglisi, S. J., Medvedev, P., Salson, M., and Chikhi, R. (2021). Data structures based on k-mers for querying large collections of sequencing data sets. *Genome Res*, 31:1–12.

Navarro, G. (2022). Indexing highly repetitive string collections, part II: compressed indexes. *ACM Comput. Surv.*, 54:26:1–26:32.

Nurk, S., Koren, S., Rhie, A., Rautiainen, M., Bzikadze, A. V., et al. (2022). The complete sequence of a human genome. *Science*, 376:44–53.

Ohno, T., Sakai, K., Takabatake, Y., I, T., and Sakamoto, H. (2018). A faster implementation of online RLBWT and its application to LZ77 parsing. *J. Discrete Algorithms*, 52-53:18–28.

Oliva, M., Rossi, M., Sirén, J., Manzini, G., Kahveci, T., et al. (2021). Efficiently merging r-indexes. In Bilgin, A., Marcellin, M. W., Serra-Sagristà, J., and Storer, J. A., editors, *31st Data Compression Conference, DCC 2021, Snowbird, UT, USA, March 23–26, 2021*, pages 203–212. IEEE.

Rossi, M., Oliva, M., Langmead, B., Gagie, T., and Boucher, C. (2022). MONI: A pangenomic index for finding maximal exact matches. *J Comput Biol*, 29:169–187.

Sekar, A., Bialas, A. R., de Rivera, H., Davis, A., Hammond, T. R., et al. (2016). Schizophrenia risk from complex variation of complement component 4. *Nature*, 530:177–83.

Shiryev, S. A. and Agarwala, R. (2024). Indexing and searching petabase-scale nucleotide resources. *Nat Methods*, 21:994–1002.

Simpson, J. T. and Durbin, R. (2012). Efficient de novo assembly of large genomes using compressed data structures. *Genome Res*, 22:549–56.

Sirén, J. (2016). Burrows-wheeler transform for terabases. In Bilgin, A., Marcellin, M. W., Serra-Sagristà, J., and Storer, J. A., editors, *2016 Data Compression Conference, DCC 2016, Snowbird, UT, USA, March 30 – April 1, 2016*, pages 211–220. IEEE.

Suzuki, H. and Kasahara, M. (2018). Introducing difference recurrence relations for faster semi-global alignment of long sequences. *BMC Bioinformatics*, 19:45.

Tatarnikov, I., Farahani, A. S., Kashgouli, S., and Gagie, T. (2023). MONI can find k-mems. In Bulteau, L. and Lipták, Z., editors, *34th Annual Symposium on Combinatorial Pattern Matching, CPM 2023, June 26–28, 2023, Marne-la-Vallée, France*, volume 259 of *LIPICS*, pages 26:1–26:14. Schloss Dagstuhl - Leibniz-Zentrum für Informatik.

Zakeri, M., Brown, N. K., Ahmed, O. Y., Gagie, T., and Langmead, B. (2024). Movi: a fast and cache-efficient full-text pangenome index. *bioRxiv*.